Fermi gas with attractive potential and arbitrary spin in a one-dimensional trap: Phase diagram for $S = \frac{3}{2}, \frac{5}{2}, \frac{7}{2}$, and $\frac{9}{2}$

P. Schlottmann[1] and A. A. Zvyagin[2,3]

[1]*Department of Physics, Florida State University, Tallahassee, Florida 32306, USA*
[2]*B. I. Verkin Institute for Low Temperature Physics and Engineering, Ukrainian National Academy of Sciences, 47 Lenin Avenue, Kharkov, UA-61103, Ukraine*
[3]*Max-Planck-Institut für Physik komplexer Systeme, DE-01187, Dresden, Germany*

A gas of ultracold ^{6}Li atoms (effective spin 1/2) confined to an elongated trap with one-dimensional properties is a candidate to display three different phases: (i) fermions bound in Cooper-pair-like states, (ii) unbound spin-polarized particles, and (iii) a mixed phase in which Cooper bound states and unpaired particles coexist. It is of great interest to extend these studies to fermionic atoms with higher spin, e.g., for neutral ^{40}K, ^{43}Ca, ^{87}Sr, or ^{173}Yb atoms. Within the grand-canonical ensemble, we investigated the μ versus H phase diagram (μ is the chemical potential and H the external magnetic field) for $S = 3/2, \ldots, 9/2$ for the ground state using the exact Bethe *ansatz* solution of the one-dimensional Fermi gas with an attractive δ-function interaction potential. There are $N = 2S + 1$ fundamental states: the particles can be either unpaired or clustered in bound states of 2, 3, ..., $2S$, and $2S + 1$ fermions. The rich phase diagram consists of these N states and various mixed phases in which combinations of the fundamental states coexist. Bound states of N fermions are not favorable in high magnetic fields, but always present if the field is low. For $S = 3/2$, possible scenarios for phase separation are explored within the local density approximation. For $S = 3/2$, the phase diagram for the superposition of a Zeeman and a quadrupolar splitting is also discussed.

PACS number(s): 71.10.Pm, 36.40.Ei, 51.30.+i

I. INTRODUCTION

Spin-imbalanced ultracold ^{6}Li atoms confined to different geometries are spin-1/2 fermion systems displaying the interplay of Cooper pairing and spin-polarization and have been the subject of several recent studies.[1–3] Confinement to nearly one-dimensional tubes can be achieved if the ultracold cloud of atoms is subjected to a two-dimensional optical lattice, which defines a two-dimensional array of tubes.[4] The tubes can be regarded as isolated if the confinement by the laser beams is strong enough to suppress tunneling between tubes. The scattering between atoms under transverse harmonic confinement is subject to a confinement-induced resonance.[5] Fine-tuning this Feshbach-type resonance, the interaction between the fermions can be made attractive and its strength can be varied.[6] The interaction is local and can be approximated by a δ-function potential in space. The confinement along the tube is roughly harmonic and weak; it can be locally incorporated into the chemical potential. Consequently, these systems of fermions are only locally homogeneous and within the local density approximation display phase separation with the variation of the chemical potential along the tube.[7,8]

One-dimensional spin-1/2 gases have been extensively studied theoretically. M. Gaudin[9] and C. N. Yang[10] extended Bethe's *ansatz* for the Heisenberg chain[11] and Lieb and Liniger's results for the locally interacting gas of bosons[12] to obtain the exact solution for a gas of spin-1/2 fermions interacting via a δ-function potential. It was shown by Gaudin[9] and later by Takahashi[13] and Lai[14] that for an attractive interaction in the ground state, there are two classes of solutions of the discrete Bethe *ansatz* equations, namely, real charge and paired complex conjugated rapidities. The former

represent spin-polarized particles and the latter correspond to bound states of the Cooper type. There are then three possible homogeneous phases at very low T, the (1) fully spin-polarized state (only real charge rapidities), (2) a phase without polarization, where all particles are bound in Cooper pairs, (only complex conjugated rapidities), and (3) a mixed phase in which unpaired spin-polarized particles coexist with Cooper pairs. The Cooper pairs are gapped (i.e., it requires a critical field to breakup the bound states) and display no long-range order. Similar results were obtained for the Hubbard model with attractive U.[15,16] The mixed phase has been interpreted[17] as the one-dimensional analog of the Fulde-Ferrell-Larkin-Ovchinnikov (FFLO) state.[18]

Tubes with ultracold gases of atoms provide the unique possibility to study fermion systems with a spin larger than 1/2, e.g., ^{40}K (spin 9/2), ^{43}Ca (spin 7/2), ^{87}Sr (spin 9/2), or ^{173}Yb (spin 5/2) atoms. With an attractive interaction, atoms with spin S can form bound states of up to $(2S + 1)$ particles, extending this way the concept of Cooper pairs to larger clusters.[19] Consequently, the phase diagram will have more possible pure and mixed phases. In this paper, we investigate the phases that can arise in the ground state using the Bethe *ansatz* solution of the one-dimensional fermion gas with δ-function potential. Sutherland[20] generalized M. Gaudin's[9] and C. N. Yang's[10] Bethe *ansatz* solution (for spin 1/2) to an arbitrary number of colors $N = 2S + 1$ [SU(N) symmetry]. For an attractive interaction, Takahashi[21] derived the integral equations for the ground-state density functions for bound states of up to $N = 2S + 1$ particles. The space extension of these bound states was further studied by C. H. Gu and C. N. Yang.[22] The classification of states, the thermodynamics, the ground-state properties, and elementary excitations of the gas have been derived by Schlottmann[23,24] for both attractive and

repulsive potential and arbitrary number of colors. Introducing different chemical potentials for each of the colors, these results are valid for an arbitrary level splitting of the N-fold multiplet.[23–25] The results for the δ-function potential model as well as other integrable models, have been extensively reviewed in Ref. 25. In this paper, we use this solution to study the phase diagram for a gas of fermionic atoms with effective spins of $S = 3/2, 5/2, 7/2$, and $9/2$ constrained to a tube. The numerical effort and the complexity of the phase diagram rapidly increase with S. As a consequence of Pauli's exclusion principle, the bound states must involve particles all with different spin components (otherwise the δ potential is not active due to nodes in the wave function). There are N basic states, namely, bound states of $N, N - 1, \ldots$, two particles, and unbound particles. The phase diagram will have many mixed phases, which can have up to N coexisting basic states. Some results of Ref. 24 were rederived in Ref. 26 for $S = 3/2$ and used to discuss the phase diagram for fixed density of particles, strong attractive coupling (Tonks-Girardeau gas limit) and Zeeman as well as quadrupolar splittings.

A two-body interaction for spin larger than $1/2$ does not necessarily have to have SU(N) symmetry. Spin-$3/2$ fermion models with contact interactions in any dimension display a generic SO(5) symmetry without tuning parameters.[27] The Hubbard variant for $S = 3/2$ has been studied via Monte Carlo algorithms in Ref. 28 and was applied to investigate the competing orders in one-dimensional optical traps in Ref. 29. Several integrable one-dimensional continuum models for the low-density limit displaying pairing have been constructed for bosonic and fermionic systems. In Ref. 30, a model for spin-1 bosons with exchange interaction is proposed and solved exactly via nested Bethe *ansätze* for the ground state and thermodynamics. An extension of this model to SO(5) symmetry for spin-$3/2$ fermions has been proposed and solved in Ref. 31; the authors obtain the thermodynamic equations and discuss the spectrum of elementary excitations. Further extensions to models with hidden Sp($2s + 1$) and SO($2s + 1$) symmetries for high spin-s fermions and bosons, respectively, can be found in Ref. 32. The influence of a pure quadratic Zeeman effect (quadrupolar splitting) on the Mott-insulator phases of hard-core one-dimensional spin-$3/2$ fermions has been studied via DMRG, leading to a rich phase diagram.[33]

There are several other theoretical studies of ultracold spin-$1/2$ atoms in one-dimension. The direct imaging of the density profiles of the spatially modulated superfluid phases in atomic fermion systems were obtained by solving the Bogoliubov-de Gennes equation.[34] The pairing states were investigated on a lattice by means of the density matrix renormalization group method in Ref. 35; this study leads to a fourth possible phase (in addition to the paired, unpaired polarized and the mixed phases) consisting of a metallic shell with free spin-down (i.e., reversed spins) fermions moving in a fully filled background of spin-up fermions. The crossover from three-dimensional (FFLO phase) to one-dimensional (mixed phase) behavior is addressed in Ref. 36, where the phase diagram for a weakly interacting array of tubes is calculated. A quantum Monte Carlo study of one-dimensional trapped fermions with attractive contact interactions was presented in Ref. 37. Finally, using the Bethe *ansatz*, the low-temperature thermodynamics was calculated in Refs. 38 and 39.

The rest of the paper is organized as follows. In Sec. II, we present the model and the discrete Bethe *ansatz* equations for periodic and open boundary conditions for fermions of arbitrary S. In Sec. III, we present the numerical solution of the Bethe *ansatz* equations for $S = 3/2$, the phase diagram for a Zeeman splitting and the local density profile along the trap. In Sec. IV, we present the numerical solution of the Bethe *ansatz* equations for spins $S = 5/2, 7/2$, and $9/2$ for a pure Zeeman splitting and the corresponding phase diagrams. In Sec. V, we investigate for $S = 3/2$ the case where in addition to the Zeeman effect there is a quadrupolar splitting. Although it is not clear if nonlinear Zeeman splittings are of relevance to ultracold atoms in one dimension, it is an instructive situation to study which has been considered in Refs. 30, 26, and 33. Conclusions are presented in Sec. VI.

II. MODEL AND BETHE ANSATZ

The Hamiltonian for a gas of nonrelativistic particles with $(2S + 1)$ colors (spin S) interacting via an attractive δ-function potential is

$$\mathcal{H} = -\sum_{i=1}^{N_p} \frac{\partial^2}{\partial x_i^2} - 2|c| \sum_{i<j} \delta(x_i - x_j) \,, \tag{1}$$

where x_i are the coordinates, N_p is the total number of particles, and c is the interaction strength. By fine tuning the confinement-induced resonance,[5] the interaction can become attractive and its strength can be varied. Here, $\hbar^2/2m$, where m is the mass of the particles, has been equated to one, or alternatively it has been scaled into $\mathcal{H}$ and c.

A. Bethe equations for periodic boundary conditions

The states of the coordinate Bethe *ansatz* are plane waves constructed from the two-particle scattering matrix. This scattering matrix satisfies the so-called Yang-Baxter triangular relation, which is a necessary condition for integrability. As a consequence of the triangular relation, many-particle scattering processes can be factorized into two-particle processes and the order in which the individual scattering processes take place can be interchanged (the order becomes arbitrary).

The generalization of the Gaudin-Yang[9,10] solution to more than two colors[20] consists of an iterative application of the Bethe-Yang hypothesis (generalized Bethe *ansatz*), such that one color is eliminated at each step, leading to $N = 2S + 1$ nested Bethe *ansätze*. Each Bethe *ansatz* gives rise to a new set of rapidities, $\{k_j\}$, $j = 1, \cdots, N_p$ for the charges (coordinate Bethe *ansatz*) and $\{\Lambda_\alpha^{(l)}\}$, $l = 1, \cdots, N - 1$, with $\alpha = 1, \cdots, M^{(l)}$ for the internal degrees of freedom (spin). Here, $M^{(l)}$ is the number of rapidities in the lth set and α is the running index within each set. All rapidities within a given set have to be different to ensure linearly independent solutions. Consider fermions of spin S with Zeeman splitting and let us denote by N_{S-m} the number of particles with spin component m. We have then $N_{S-m_1} \geqslant N_{S-m_2}$ if $m_1 > m_2$ and define

$$M^{(i)} = \sum_{m=-S+i}^{S} N_{S+m}, \quad M^{(0)} = N_p, \quad M^{(2S+1)} = 0, \tag{2}$$

such that $N_p \geqslant M^{(1)} \geqslant \cdots \geqslant M^{(2S)} \geqslant 0$. As a consequence of the SU(N) invariance of the model, the nested Bethe *ansätze* for periodic boundary conditions yield the following sets of coupled equations:[20,23,25]

$$\exp(ik_jL) = \prod_{\beta=1}^{M^{(1)}} e\big(k_j - \Lambda_\beta^{(1)}\big), \quad j = 1, \ldots, N_p, \quad (3)$$

$$\prod_{\beta=1}^{M^{(l-1)}} e\big(\Lambda_\alpha^{(l)} - \Lambda_\beta^{(l-1)}\big) \prod_{\beta=1}^{M^{(l+1)}} e\big(\Lambda_\alpha^{(l)} - \Lambda_\beta^{(l+1)}\big)$$

$$= -\prod_{\beta=1}^{M^{(l)}} e\big[\big(\Lambda_\alpha^{(l)} - \Lambda_\beta^{(l)}\big)/2\big], \alpha = 1, \ldots, M^{(l)}$$

$$l = 1, \ldots, 2S, \quad (4)$$

where

$$e(x) = \frac{x - i\frac{1}{2}|c|}{x + i\frac{1}{2}|c|}, \quad (5)$$

$\Lambda_j^{(0)} \equiv k_j$, and L is the length of the box. The energy and the momentum of the state are given by

$$E = \sum_{j=1}^{N_p} k_j^2, \quad P = \sum_{j=1}^{N_p} k_j. \quad (6)$$

B. Bethe equations for open boundary conditions

Equations (3) and (4) are derived for the standard periodic boundary conditions. Tubes, however, are not periodic and better represented by open or reflecting boundary conditions. A particle reaching the boundary is then reflected undergoing $k_j \rightarrow -k_j$ but without changing its energy. The corresponding reflection matrix satisfies reflection equations with the two-particle scattering matrix, extending the Yang-Baxter equations. All matrices can be diagonalized simultaneously.[40,41] The total length of a period is now $2L$, where L is the length of the trap. It is convenient to write the Bethe equations in a form similar to Eq. (4) by letting the indices j and α run from $-N_p$ to N_p and $-M^{(l)}$ to $M^{(l)}$, respectively.[42,43] The Bethe *ansatz* equations for open boundary conditions are then

$$\exp(i2k_jL)e(k_j) = \prod_{\beta=-M^{(1)}}^{M^{(1)}} e\big(k_j - \Lambda_\beta^{(1)}\big),$$

$$j = -N_p, \ldots, N_p, \quad (7)$$

$$e\big[\big(\Lambda_\alpha^{(l)}/2\big)\big] \prod_{\beta=-M^{(l-1)}}^{M^{(l-1)}} e\big(\Lambda_\alpha^{(l)} - \Lambda_\beta^{(l-1)}\big)$$

$$\times \prod_{\beta=-M^{(l+1)}}^{M^{(l+1)}} e\big(\Lambda_\alpha^{(l)} - \Lambda_\beta^{(l+1)}\big) = -\big[e\big(\Lambda_\alpha^{(l)}\big)\big]^2$$

$$\times \prod_{\beta=-M^{(l)}}^{M^{(l)}} e\big[\big(\Lambda_\alpha^{(l)} - \Lambda_\beta^{(l)}\big)/2\big], \alpha = -M^{(l)}, \ldots, M^{(l)},$$

$$l = 1, \ldots, 2S. \quad (8)$$

Hence, there are twice as many rapidities and the box is also twice as large, leaving the density of rapidities unchanged. The main difference between open and periodic boundary conditions is then the independent factors in Eqs. (7) and (8), which contribute with $1/L$ terms to the rapidity densities. This is very similar to the effect of magnetic impurities in a chain. Also, for periodic boundary conditions, the Bethe states are plane waves, while for open boundary conditions they are standing waves. The energy and momentum are still given by Eq. (6). The open boundary Bethe equations for the present model were derived previously by Oelkers *et al.*[44]

C. Classification of states and energy potentials

For an attractive interaction and large L, the solutions of the discrete Bethe equations can be classified according to (i) real charge rapidities, belonging to the set $\{k_j\}$, associated with unpaired propagating spin-polarized particles, (ii) complex spin and charge rapidities, which correspond to bound states of particles with different spin components, and (iii) strings of complex spin rapidities, which represent bound spin states.[23,25] States in class (iii) are not represented in the ground state; these states correspond to excited states and are not considered here. This classification of states is completely analogous to that of the Anderson impurity of arbitrary spin in the $U \rightarrow \infty$ limit[45] (see also Refs. 46–49) and the one-dimensional degenerate supersymmetric t-J model.[50]

Since only particles with different spin components are scattered, i.e., experience an effective attractive interaction, we may build bound states of up to $(2S + 1)$ particles. A bound state of n ($n \leqslant N = 2S + 1$) is characterized by one real $\xi^{(n-1)}$ rapidity and, in general, complex $\Lambda^{(l)}$ rapidities, $l < n - 1$, given by[21]

$$\Lambda_p^{(l)} = \xi^{(n-1)} + ip|c|/2, \quad l \leqslant n - 1 \leqslant 2S,$$

$$p = -(n - l - 1), -(n - l - 3), \ldots, (n - l - 1). \quad (9)$$

These spin and charge strings form classes (i) and (ii), which are present in the ground state.[23] The real rapidities $\xi^{(n-1)}$ have all to be different and satisfy the Fermi-Dirac statistics, i.e., the states are either occupied or empty. (For $S = 1/2$, the bound states are frequently called Cooper pairs, although this analogy is not rigorous.) In the ground state, the rapidities are densely distributed in the interval $[-B_l, B_l]$ and we denote with $\varepsilon^{(l)}(\xi)$, $l = 0, 1, \ldots, 2S$, the dressed energy potentials (entering the Fermi-Dirac distribution). The $N = 2S + 1$ energy potentials satisfy the following coupled linear integral equations:[24,25]

$$\varepsilon^{(l)}(\xi) = D_l(\xi) - \sum_{q=0}^{2S} \int_{-B_q}^{B_q} d\xi' K_{lq}(\xi - \xi')\varepsilon^{(q)}(\xi'), \quad (10)$$

where the $D_l(\xi)$ are the driving terms and $K_{lq}(\xi)$ the integration kernel. The kernel can be written in a compact form:[24]

$$K_{lq}(\xi) = \int \frac{d\omega}{2\pi} \exp[i\xi\omega - (l + q - p_{l,q})|\omega c|/2]$$

$$\times \sinh[(p_{l,q} + 1)\omega c/2] \big/ \sinh(\omega c/2), \quad (11)$$

where $p_{l,q} = \min(l,q) - \delta_{l,q}$. Note that $K_{lq}(\xi) = K_{ql}(\xi)$. The driving terms are given by[24,25]

$$D_l(\xi) = (l+1)\left[\xi^2 - \frac{l(l+2)}{12}c^2 - \mu_l\right], \qquad (12)$$

where μ_l is the chemical potential for the bound states involving $(l+1)$ particles. The μ_l determine the integration limits B_l through the condition that $\varepsilon^{(l)}(\pm B_l) = 0$, since occupied states correspond to $\varepsilon^{(l)}(\xi) < 0$, and for empty states, the quantity is positive. For a pure Zeeman splitting, we obtain

$$\mu_l = \mu + \frac{2S - l}{2}H. \qquad (13)$$

Here, μ and H are the chemical potential and the Zeeman splitting, playing the role of the Lagrange parameters for the conservation of the total number of particles and the magnetization.

In terms of

$$a_n(x) = \frac{1}{\pi}\frac{n|c|/2}{x^2 + n^2c^2/4} \qquad (14)$$

the kernel for $S = 3/2$ reduces to

$$\begin{aligned}
&K_{00} = 0, \ K_{01} = a_1, \ K_{02} = a_2, \ K_{03} = a_3, \\
&K_{11} = a_2, \ K_{12} = a_1 + a_3, \ K_{13} = a_2 + a_4, \\
&K_{22} = a_2 + a_4, \ K_{23} = a_1 + a_3 + a_5, \\
&K_{33} = a_2 + a_4 + a_6.
\end{aligned} \qquad (15)$$

Note that if all the $\varepsilon^{(l)}$ in Eq. (10) are rescaled to $\varepsilon^{(l)}/c^2$, μ to μ/c^2, H to H/c^2, all B_l to $B_l/|c|$, and ξ to $\xi/|c|$, the equations are universal, i.e., independent of the magnitude of $|c|$. Hence, within the framework of the grand canonical ensemble, without loss of generality, it is sufficient to present the results for $|c| = 1$. The problem has then only two independent parameters, namely, H and μ.

An ultracold atom system is inherently inhomogeneous since the diameter of the tube gradually changes with position from the center of the trap to its boundaries. As a consequence of the changing diameter of the tube, the quantization in the plane transversal to the tube gradually changes the zero of energy. This change can be represented by a harmonic potential of frequency ω_{ho}, so that the actual local chemical potential μ is a function of x given by

$$\mu(x) + \frac{1}{2}m\omega_{ho}^2 x^2 = \text{const.} \qquad (16)$$

Within the local density approximation, it is $\mu(x)$ that enters the Bethe equations (10)–(13). The solution is then exact for the one-dimensional system, but approximate for the trap. This approximation[4,7,8] is expected to be good since the variation of μ with x is slow. The approximation neglects the quantization of the harmonic confinement, which is treated classically and locally incorporated into the chemical potential.

Fluctuations in the particle density arise due to the x dependence of μ and due to possible weak Josephson tunneling between tubes. It is then necessary to solve the Bethe equations in the grand canonical ensemble rather than for the canonical ensemble, i.e., at constant number of particles. The results within the canonical ensemble are not universal, because the constraint of fixed number of particles invalidates the scaling with $|c|$ discussed above. The above integral equations for

$S = 3/2$ were solved for constant number of particles in Ref. 26.

III. PHASE DIAGRAM FOR $S = 3/2$ FOR ZEEMAN SPLITTING

In this section, we discuss the phase diagram for a pure Zeeman splitting of the levels for the case $S = 3/2$. The set of equations (10)–(13) is solved numerically by iteration. In this case, the energy potential $\varepsilon^{(0)}$ corresponds to unpaired particles with spin-component $S_z = 3/2$, the energy $\varepsilon^{(1)}$ to bound pairs with spin-components $S_z = 3/2$ and $S_z = 1/2$, the potential $\varepsilon^{(2)}$ to bound states of three particles of spin components $S_z = 3/2$, $S_z = 1/2$, and $S_z = -1/2$, respectively; and finally, $\varepsilon^{(3)}$ to bound states of four particles all with different spin components. We denote these states with roman numbers, I, II, III, and IV, respectively. These states can coexist in mixed phases, for example, we denote with I + IV the coexistence of unpaired and bound states of four particles and with I + II + III a phase where all states except four-particle bound states are present.

The phase diagram of $\mu(x)$ versus H for $|c| = 1$ and $S = 3/2$ is shown in Fig. 1. Other values of $|c|$ can be reduced to this phase diagram by adequately scaling μ and H. Note that all phase boundaries are given by the zero of some energy potential. The phase boundaries are then crossover lines, which are accompanied by a square-root singularity of one of the densities of states (one-dimensional van Hove singularity) in analogy to a Prokovskii-Talapov transition.[51] For small magnetic fields, all particles are bound in four-particle bound states (generalized Cooper pairs). The shaded area is the region where all bands are empty (system without particles). With increasing field, other phases become realized. At very large magnetic fields and/or for low values of μ (small number of particles), the phase IV is not favorable. For large μ and intermediate magnetic fields, all four bands are
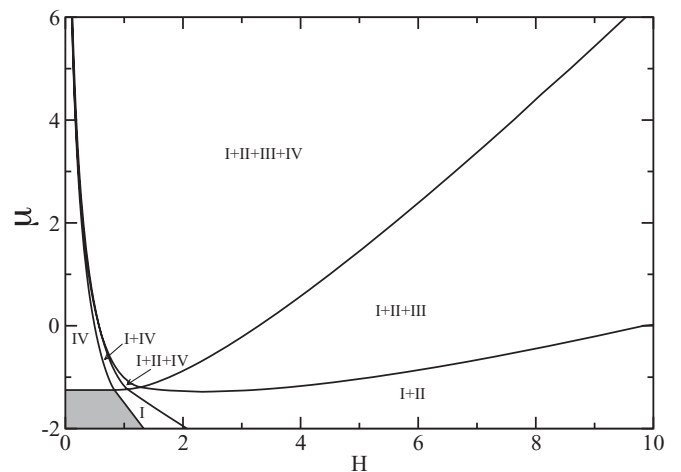

FIG. 1. Ground-state phase diagram μ vs H for a homogeneous fermion gas of spin $S = 3/2$ with $|c| = 1$. The shaded area corresponds to the empty system (no particles). The roman numbers denote the number of particles involved in a bound state. Regions with more than one roman number are mixed phases with coexisting bound states. Note that in the vertical axis, μ is a function of x as given by Eq. (16).
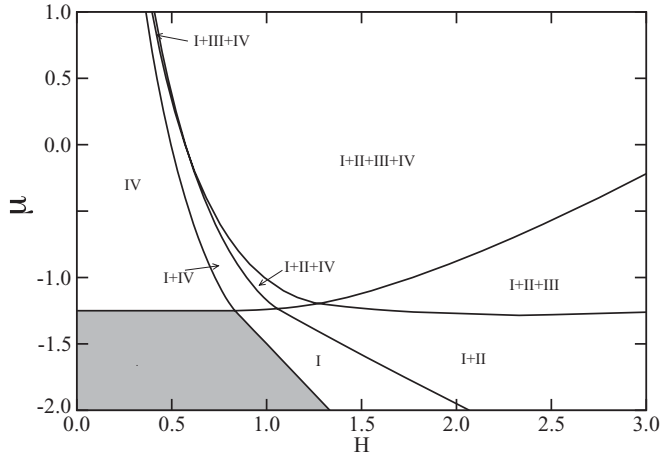
FIG. 2. Expanded view of the ground-state phase diagram μ vs H of Fig. 1 for a homogeneous fermion gas of spin $S = 3/2$ with $|c| = 1$ to show the multiple phases for the low-density region. The shaded area corresponds to the empty system (no particles).
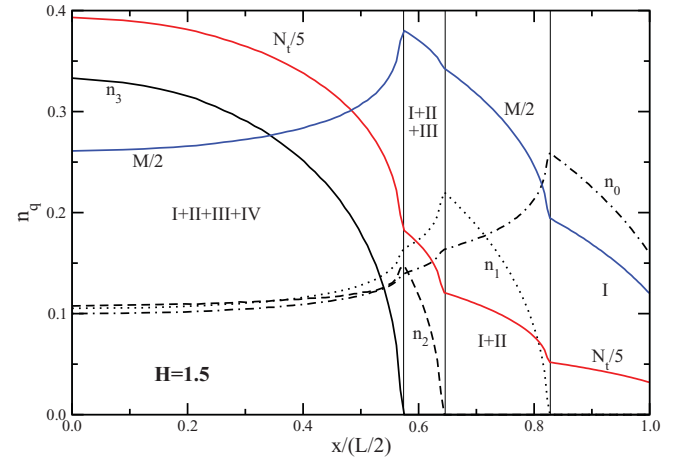

FIG. 3. (Color online) Density profile within the local density approximation for $H = 1.5$, $\mu(0) = -0.7$, $\mu(L/2) = -2.0$, and $S = 3/2$. The position along the trap is given by Eq. (17). The three crossovers between phases are shown by the thin vertical lines. The densities n_q of bound states of $q + 1$ particles (or polarized unbound particles if $q = 0$) are given by the solid (n_3), dashed (n_2), dotted (n_1), and dash-dotted (n_0) curves. The density of the total number of particles N_t (red curve) and the magnetization density M (blue curve) as a function of x are also shown. Note that the scales of N_t and M are reduced by a factor of five and two, respectively.

populated and hence spin-polarized unbound particles coexist with all possible bound states. This phase diagram can be compared to the one obtained in Ref. 26 (Figs. 3 and 4) for fixed number of particles (canonical ensemble). For a pure Zeeman splitting and as a function of field, these authors obtain crossovers from phase IV to I + IV to I. A constant number of particles corresponds to a curve $\mu(H)$ in Fig. 1. The strong-interaction limit considered in Ref. 26 corresponds to a low particle density. The sequence of phases we then expect from Fig. 1 is also IV to I + IV to I, in agreement with Ref. 26.

Figure 2 shows the expanded view of the region for small μ and H, which displays multiple crossovers. For larger μ, there is a small region where the phase I + III + IV is stable. As mentioned above, the harmonic confinement of the trap can be treated quasi-classically and can be absorbed into the chemical potential via Eq. (16).[52] The chemical potential then decreases as we move from the center of the trap toward the boundaries. Hence we move downward along a vertical line on the phase diagram. This can give rise to phase separation along the length of the trap. For instance, for $H = 2$ for a sufficiently high density of atoms, at the center of the trap the phase with all bound states coexisting (I + II + III + IV) would be favored, then moving toward the end points (in either direction) of the trap, first the four-particle bound states disappear (phase I + II + III), then the bound states of three particles (phase III) are depopulated and polarized unbound particles coexist with bound pairs (phase I + II), and finally a fully polarized gas phase (I) is possible. For $H = 1$, on the other hand, we again could have the I + II + III + IV phase at the center of the trap and by moving to the boundaries we would observe the I + II + IV mixed phase, then the I + IV phase and finally unbound fully polarized atoms (I).

The local density profile as a function of x for the different phases for $H = 1.5$ is displayed in Fig. 3, where Eq. (16) was used to parametrize the chemical potential in a trap of length L. Given $\mu(0)$ and $\mu(L/2)$, i.e., the chemical potential at the

center and boundary of the trap, the position along the trap is given by [from Eq. (16)]

$$x/(L/2) = \sqrt{[\mu(x) - \mu(0)]/[\mu(L/2) - \mu(0)]} \ . \quad (17)$$

The density function of the rapidities is obtained from the dressed energies $\varepsilon^{(q)}(\xi)$ by differentiation with respect to μ, i.e.,[24,25]

$$\rho_h^{(q)}(\xi) + \rho^{(q)}(\xi) = -\frac{1}{2\pi} \frac{\partial \varepsilon^{(q)}(\xi)}{\partial \mu}, \quad (18)$$

where $\rho^{(q)}(\xi)$ is the particle density and $\rho_h^{(q)}(\xi)$ the corresponding hole density for bound states involving $q + 1$ particles. The integral equations satisfied by the density functions are similar to the ones for the dressed energy potentials, i.e., the integration kernel and the integration limits are the same, but the driving terms are $D_l = (l + 1)/(2\pi)$.[21] After solving these equations numerically, the number of bound states (or polarized unbound particles if $q = 0$) per unit length are obtained from

$$n_q = \int_{-B_q}^{B_q} d\xi \rho^{(q)}(\xi) \ , \quad (19)$$

Note that as a function of μ the densities vanish with a square-root singularity that is characteristic of one-dimensional van Hove singularities as can be seen in Fig. 3. The density of the total number of particles is given by $N_t = \sum_{q=0}^{2S}(q + 1)n_q$ and the magnetization density by $M = (1/2)\sum_{q=0}^{2S}(q + 1)(2S - q)n_q$. Both quantities are displayed in Fig. 3 (red and blue curves, respectively) for the phase separation along the trap. They also show the square root singularities, consequences of the van Hove singularities in the densities, as a function of μ each time there is a level crossing.
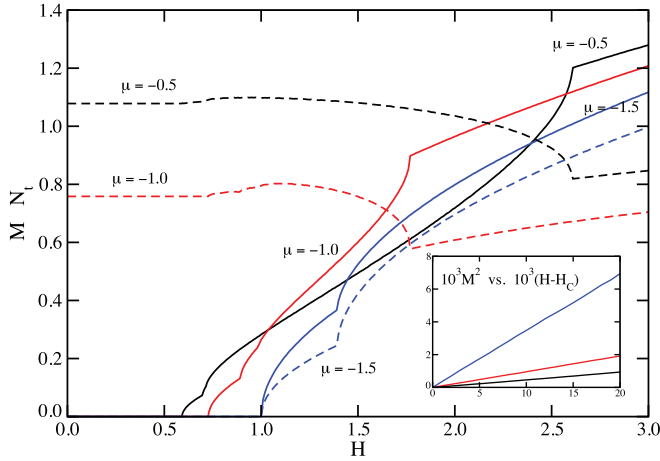
FIG. 4. (Color online) Density of total number of particles N_t (dashed) and the magnetization density M (solid) for $S = 3/2$ as a function of magnetic field for three values of μ: $\mu = -0.5$ (black), $\mu = -1.0$ (red), and $\mu = -1.5$ (blue). At the crossovers from one phase to another, a van Hove singularity is seen in both N_t and M. The onset of the magnetization is proportional to $(H - H_C)^{1/2}$ with the critical field depending on μ. This is seen in the inset where M^2 is plotted vs $H - H_C$, yielding a straight line in all three cases.

The density of the total number of particles N_t and the magnetization density M as a function of magnetic field for $S = 3/2$ and three values of μ is shown in Fig. 4. Every level crossing is accompanied by a square-root dependence due to the one-dimensional van Hove singularity in the density of states. The onset of the magnetization is at a critical field H_C that depends on μ. In the inset of Fig. 4, we plot M^2 versus $H - H_C$, which follows a straight line, proving the square root dependence of the magnetization. We can then conclude that the transitions are level crossings, consequence of a band being emptied, and independent on how the transition is crossed (along μ or H or any straight line $\mu = aH + b$) it will give rise to a square-root singularity in the density of states. These transitions are level crossings of the Prokovskii-Talapov type.[51] These conclusions are valid within the grand canonical ensemble and a consequence that the dressed energy potentials are all quadratic in the rapidity.

IV. PHASE DIAGRAM FOR SPIN $S = 5/2, 7/2$, AND $9/2$

In this section, we extend the solution of Eqs. (10)–(13) to spins larger than 3/2. The procedure is quite similar to that of $S = 3/2$, but the numerical effort grows rapidly with N, since there are now N dressed energy potentials coupled by the system of integral equations. The number of possible phases, especially the mixed phases, also increases rapidly with N. The phases are again denoted by roman letters and the empty phases (no particles) is denoted by zero. The results are shown in Figs. 5 ($S = 5/2$), 6 ($S = 7/2$), and 7 ($S = 9/2$).

Several common trends emerge by comparing Figs. 2 and 5–7. There are $2S$ nearly parallel boundary lines starting almost vertically at the top of the phase diagram, which then have a curvature to the right and leave the panels either at the bottom right or the right side. These curves correspond to the zeros of the dressed energy potentials $\varepsilon^{(l)}$ for $l = 0, \ldots, 2S - 1$,
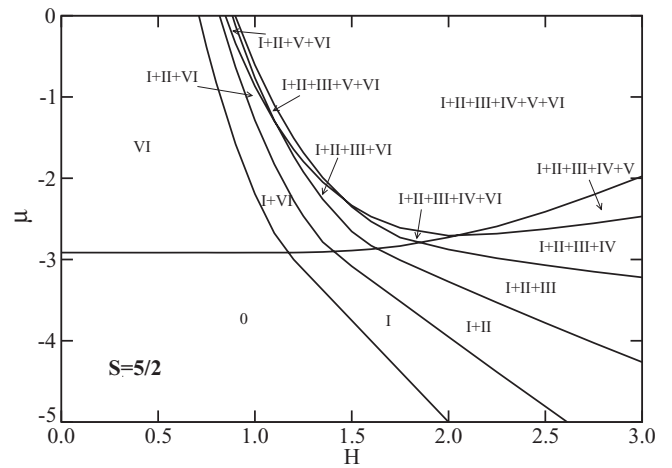
i.e., the states that are magnetic field dependent. The zero of $\varepsilon^{(2S)}$, which corresponds to bound states of N particles and is nonmagnetic, is the almost horizontal curve starting at the left and leaving the panel at the right. This curve divides the phase diagrams into two parts, namely, below that curve, there are no clusters of N particles and above, these clusters are always present.

At small fields, the system either has no particles (below the $\varepsilon^{(2S)} = 0$ line) or only bound states of N particles (above that line). With increasing field then first unpaired particles
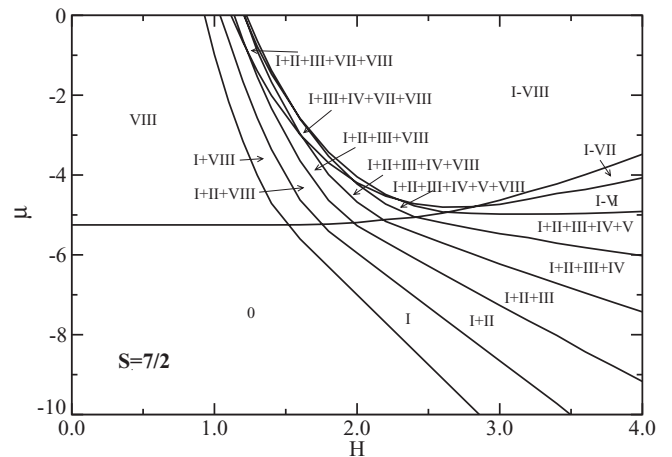

FIG. 5. Ground-state phase diagram μ vs H for a homogeneous fermion gas of spin $S = 5/2$ with $|c| = 1$. The empty system (no particles) in the lower left corner is denoted with 0. The Roman numbers denote the number of particles involved in a bound state. Regions with more than one roman number are mixed phases with coexisting bound states. Note that in the vertical axis, μ is a function of x as given by Eq. (16).

FIG. 6. Ground-state phase diagram μ vs. H for a homogeneous fermion gas of spin $S = 7/2$ with $|c| = 1$. The empty system (no particles) in the lower left corner is denoted with zero. The roman numbers denote the number of particles involved in a bound state. Regions with more than one roman number are mixed phases with coexisting bound states. For instance, the notation I–VI is a short-hand notation for I + II + III + IV + V + VI, in which the phases from I to VI coexist. Note that in the vertical axis, μ is a function of x as given by Eq. (16).
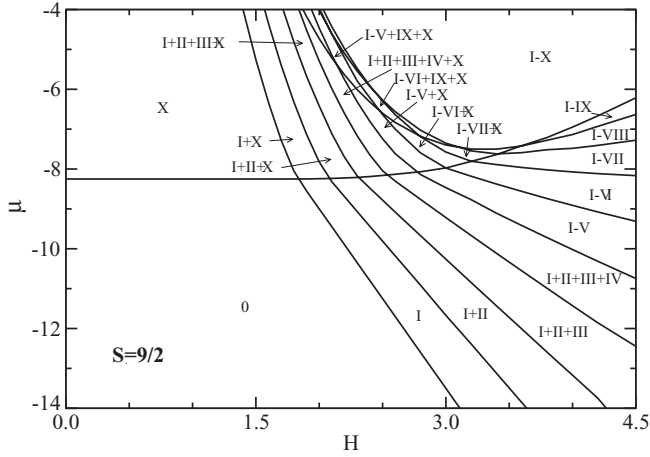
FIG. 7. Ground-state phase diagram μ vs H for a homogeneous fermion gas of spin $S = 9/2$ with $|c| = 1$. The empty system (no particles) in the lower left corner is denoted with zero. The roman numbers denote the number of particles involved in a bound state. Regions with more than one roman number are mixed phases with coexisting bound states. For instance, the notation I–VI is a short-hand notation for $I + II + III + IV + V + VI$, in which the phases from I to VI coexist. Note that in the vertical axis, μ is a function of x as given by Eq. (16).

(spin-component $S_z = S$) emerge, then paired particles (spin-components $S_z = S$ and $S_z = S - 1$) coexisting with unpaired particles (and clusters of N particles if above the $\varepsilon^{(2S)} = 0$ line), this is followed by the addition of bound states of three particles, etc. This pattern is only changed above the $\varepsilon^{(2S)} = 0$ line when many bound states coexist, due to several line crossings. In the upper right corner of the phase diagrams, a phase with all bound states coexisting is stable. This pattern of the phase diagrams found for $S \leqslant 9/2$ is not expected to change for spins larger than $9/2$.

V. PHASE DIAGRAM FOR $S = 3/2$ WITH ZEEMAN AND QUADRUPOLAR SPLITTING

For $S > 1/2$, level splittings other than the Zeeman effect are possible. Here, we consider a quadrupolar splitting superimposed with the Zeeman effect. Nonlinear Zeeman splittings have been considered previously[26,33] in similar contexts. In particular, in Ref. 26, Bethe *ansatz* equations for the same model but a fixed number of particles (canonical ensemble) were employed, while in the present paper, we consider the grand canonical ensemble (variable number of particles). For $S = 3/2$, the Zeeman and quadrupolar splittings are not the most general case, since also octupolar splittings are possible. It is not clear if such a situation (quadrupolar and octupolar splittings) can be realized experimentally for ultracold atoms in 1D, but the problem is theoretically sufficiently interesting to be addressed.

The Hamiltonian for the level splitting is given by

$$\mathcal{H}_{spl} = -HS_z + D\left[3S_z^2 - S(S+1)\right], \tag{20}$$

where D can be either positive or negative. To be specific, we consider again the case $S = 3/2$. Note that the Hamiltonian (1) commutes with $\mathcal{H}_{spl}$, so that the Bethe states also diagonalize

$\mathcal{H} + \mathcal{H}_{spl}$. Keeping D fixed and as a function of H, $\mathcal{H}_{spl}$ displays two level crossings; hence, we need to consider three regions, namely, region (i) $(H \leqslant 3|D|)$, region (ii) $(3|D| \leqslant H \leqslant 6|D|)$, and region (iii) $(6|D| \leqslant H)$. For $D > 0$, the bound states I, II, III, and IV are then composed by particles with the following S_z components; in region (i), $(1/2)$, $(1/2, -1/2)$, $(1/2, -1/2, 3/2)$, and $(1/2, -1/2, 3/2, -3/2)$, respectively, in region (ii), $(1/2)$, $(1/2, 3/2)$, $(1/2, 3/2, -1/2)$, and $(1/2, 3/2, -1/2, -3/2)$, respectively, and in region (iii), $(3/2)$, $(3/2, 1/2)$, $(3/2, 1/2, -1/2)$, and $(3/2, 1/2, -1/2, -3/2)$, respectively. Region (iii) is then similar to the case of a pure Zeeman splitting. Hence at the crossovers, the character of the bound states changes. The corresponding chemical potentials μ_i in Eqs. (10)–(13) are then

for region (i) $(H \leqslant 3D)$:
$$\mu_0 = \mu + 3D + 3H/2,$$
$$\mu_1 = \mu + 3D$$
$$\mu_2 = \mu + D + H/6,$$
$$\mu_3 = \mu,$$
for region (ii) $(3D \leqslant H \leqslant 6D)$:
$$\mu_0 = \mu + 3D + 3H/2,$$
$$\mu_1 = \mu + H$$
$$\mu_2 = \mu + D + H/6,$$
$$\mu_3 = \mu,$$
and for region (iii) $(6D \leqslant H)$:
$$\mu_0 = \mu + 3D + 3H/2,$$
$$\mu_1 = \mu + H$$
$$\mu_2 = \mu - D + H/2,$$
$$\mu_3 = \mu.$$

Similarly, one can obtain the chemical potentials for $D < 0$. The procedure is completely analogous to that used for
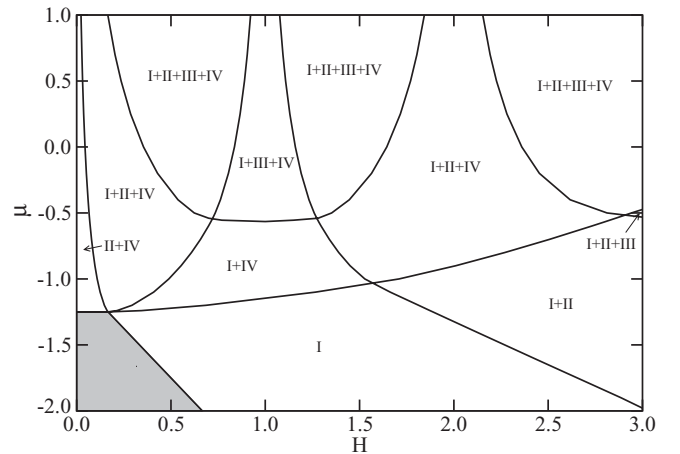

FIG. 8. Ground-state phase diagram μ vs H for a homogeneous fermion gas of spin $S = 3/2$ with $|c| = 1$ and a quadrupolar splitting $D[3S_z^2 - S(S+1)]$ for $D = 1/3$. The shaded area corresponds to the empty system (no particles). Level crossings of the Zeeman and quadrupolar terms occur at $H = 3D$ and $6D$.

FIG. 9. Ground-state phase diagram μ vs H for a homogeneous fermion gas of spin $S = 3/2$ with $|c| = 1$ and a quadrupolar splitting $D[3S_z^2 - S(S + 1)]$ for $D = -1/3$. The shaded area corresponds to the empty system (no particles). Level crossings of the Zeeman and quadrupolar terms occur at $H = 3|D|$ and $6|D|$.
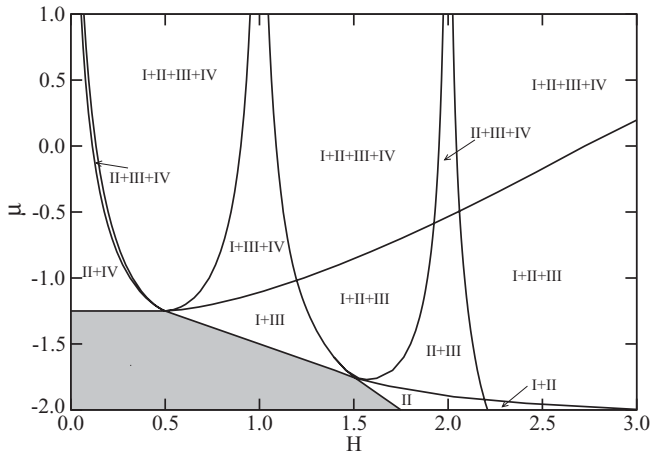
magnetic impurities (degenerate Anderson model in the $U \rightarrow \infty$ limit with Zeeman and crystalline field splittings).[49]

The phase diagram for $D = 1/3$ and $-1/3$ is shown in Figs. 8 and 9, respectively. For these parameters the level crossings are at $H = 1$ and $H = 2$. The level crossings stabilize the I + III + IV and I + II + IV (II + III + IV) mixed phases over the I + II + III + IV mixed phase. As discussed above, the phase I + III + IV for $H \geqslant 1$ involves different condensates than for $H \leqslant 1$. All phase boundaries are the consequence of one of the four rapidity bands getting empty and, hence, a transition involves a one-dimensional van Hove singularity with the corresponding consequences on the density of states and low-T specific heat. For small magnetic fields, the phase is a mixture of two-particle and four-particle bound states. For larger fields H, the four-particle bound states are only favorable if the density of particles is high enough. Also for intermediate magnetic fields the phase diagram for $D > 0$ is very different from that of $D < 0$.

VI. CONCLUSIONS

We studied an ultracold gas of fermionic atoms with an attractive contact potential by solving the corresponding Bethe *ansatz* equations. We obtained the phase diagram for $S = 3/2$, $5/2$, $7/2$, and $9/2$ in a magnetic field (μ versus H) within the grand canonical ensemble. For $S = 3/2$, four elementary states can occur: (i) polarized unbound atoms with spin-component $S_z = 3/2$, (ii) bound pairs of atoms with spin-components $S_z = 3/2$ and $S_z = 1/2$, (iii) bound states of three particles

with spin-components $S_z = 3/2$, $S_z = 1/2$, and $S_z = -1/2$, and (iv) bound states of four particles, one with each spin component. For a general S, there are $N = 2S + 1$ such elementary states. Mixed phases of different classes of bound states dominate the phase diagram. For a given chemical potential, the phases are homogeneous and display no long-range order. The transitions between phases are crossovers of the Prokovskii-Talapov type.[51]

There are several advantages of working in the grand-canonical ensemble with fixed chemical potential, rather than with a fixed number of particles.[26] (1) By rescaling all quantities in the integral equations for the dressed energy potentials, $\varepsilon^{(q)}$, with the interaction strength $|c|$, one obtains universal equations for the phase diagram μ versus H. Our phase diagram shown in Figs. 1, 2, and 5–7 is then valid for all attractive $|c|$. This is not the case if the total number of particles is kept fixed. (2) From the general trends for $S \leqslant 9/2$, we can draw conclusions of the μ versus H phase diagram valid for all spins. (3) Since the diameter of the tube gradually changes with position from the center of the trap to its boundaries, the effective local chemical potential varies along the tube. Within the local density approximation this change can be represented by a harmonic potential and as a consequence of the x dependence of μ there is an inherent tendency of phase separation,[4] i.e., the trap is inhomogeneous. At different positions of the trap then different phases may be realized and a sequence of transitions should be observed along the trap. (4) Josephson tunneling between tubes and interactions between particles in different tubes,[17,36] may give rise to a dimensional crossover from one dimension to a higher dimension. This gives rise to long-range order of quantities that are generalizations of Cooper pairs for $S = 1/2$ to higher spin. The system remains strongly anisotropic and pure (there are almost no impurities) and is hence favorable for inhomogeneities like modulations of the order parameter of the FFLO type in the presence of an external magnetic field.

For $S = 3/2$, we also investigated the interesting situation of a quadrupolar splitting superimposed with the Zeeman field. In this case, the spin energy levels display two crossovers as a function of the magnetic field. Hence the character of the bound states before and after the crossover changes. In general, bound states of four particles are not favorable for low particle density or high magnetic fields.

[1] M. W. Zwierlein, A. Schirotzek, C. H. Schunck, and W. Ketterle, Science **311**, 492 (2006); Nature (London) **442**, 54 (2006).

[2] Y. Shin, M. W. Zwierlein, C. H. Schunck, A. Schirotzek, and W. Ketterle, Phys. Rev. Lett. **97**, 030401 (2006); C. H. Schunck, Y. Shin, A. Schirotzek, M. W. Zwierlein, and W. Ketterle, Science **316**, 867 (2007).

[3] G. B. Partridge, W. H. Li, R. I. Kamar, Y. A. Liao, and R. G. Hulet, Science **311**, 503 (2006); G. B. Partridge, W. H. Li, Y. A. Liao, R. G. Hulet, M. Haque, and H. T. C. Stoof, Phys. Rev. Lett. **97**, 190407 (2006).

[4] Y. A. Liao, A. S. C. Rittner, T. Paprotta, W. H. Li, G. B. Partridge, R. G. Hulet, S. K. Baur, and E. J. Mueller, Nature (London) **467**, 567 (2010).

[5] M. Olshanii, Phys. Rev. Lett. **81**, 938 (1998).

[6] T. Bergeman, M. G. Moore, and M. Olshanii, Phys. Rev. Lett. **91**, 163201 (2003).

[7] G. Orso, Phys. Rev. Lett. **98**, 070402 (2007).

[8] H. Hu, X.-J. Liu, and P. D. Drummond, Phys. Rev. Lett. **98**, 070403 (2007).

[9] M. Gaudin, Phys. Lett. A **24**, 55 (1967).

[10] C. N. Yang, Phys. Rev. Lett. **19**, 1312 (1967).

[11] H. A. Bethe, Z. Phys. **71**, 205 (1931).

[12] E. H. Lieb and W. Liniger, Phys. Rev. **130**, 1605 (1963).

[13] M. Takahashi, Prog. Theor. Phys. **46**, 1388 (1971).

[14] C. K. Lai, Phys. Rev. Lett. **26**, 1472 (1971); Phys. Rev. A **8**, 2567 (1973).

[15] T. B. Bahder and F. Woynarovich, Phys. Rev. B **33**, 2114 (1986).

[16] Kong-Ju-Bock Lee and P. Schlottmann, Phys. Rev. B **40**, 9104 (1989).

[17] K. Yang, Phys. Rev. B **63**, 140511(R) (2001).

[18] P. Fulde and A. Ferrell, Phys. Rev. **135**, A550 (1964); A. Larkin and Y. N. Ovchinnikov, Zh. Eksp. Teor. Fiz. **47**, 1136 (1964) [Sov. Phys. JETP **20**, 762 (1965)].

[19] This is known for nucleons that have a pseudospin in addition to the spin; α-particles are bound states of four nucleons, the nuclei of ^{3}He and tritium are examples of bound states of three nucleon and the nucleus of deuterium binds two nucleons.

[20] B. Sutherland, Phys. Rev. Lett. **20**, 98 (1968).

[21] M. Takahashi, Prog. Theor. Phys. **44**, 899 (1970).

[22] C. H. Gu and C. N. Yang, Commun. Math. Phys. **122**, 105 (1989).

[23] P. Schlottmann, J. Phys. Condens. Matter **5**, 5869 (1993).

[24] P. Schlottmann, J. Phys. Condens. Matter **6**, 1359 (1994).

[25] P. Schlottmann, Int. J. Mod. Phys. B **11**, 355 (1997).

[26] X. W. Guan, M. T. Batchelor, C. Lee, and J. Y. Lee, Europhys. Lett. **86**, 50003 (2009).

[27] C. Wu, J.-P. Hu, and S.-C. Zhang, Phys. Rev. Lett. **91**, 186402 (2003).

[28] C. Wu and S.-C. Zhang, Phys. Rev. B **71**, 155115 (2005).

[29] C. Wu, Phys. Rev. Lett. **95**, 266404 (2005).

[30] J. Cao, Y. Jiang, and Y. Wang, Europhys. Lett. **87**, 30005 (2007).

[31] Y. Jiang, J. Cao, and Y. Wang, Europhys. Lett. **79**, 10006 (2009).

[32] Y. Jiang, J. Cao, and Y. Wang, J. Phys. A: Math. Theor. **44**, 345001 (2011).

[33] K. Rodriguez, A. Argüelles, M. Colomé-Tatché, T. Vekua, and L. Santos, Phys. Rev. Lett. **105**, 050402 (2010).

[34] T. Mizushima, K. Machida, and M. Ichioka, Phys. Rev. Lett. **94**, 060404 (2005).

[35] A. E. Feiguin and F. Heidrich-Meisner, Phys. Rev. B **76**, 220508 (2007).

[36] M. M. Parish, S. K. Baur, E. J. Mueller, and D. A. Huse, Phys. Rev. Lett. **99**, 250403 (2007).

[37] M. Casula, D. M. Ceperley, and E. J. Mueller, Phys. Rev. A **78**, 033607 (2008).

[38] X. W. Guan, M. T. Batchelor, C. Lee, and M. Bortz, Phys. Rev. B **76**, 085120 (2007).

[39] P. Kakashvili and C. J. Bolech, Phys. Rev. A **79**, 041603(R) (2009).

[40] E. K. Sklyanin, J. Phys. A **21**, 2375 (1988).

[41] P. Fendley and H. Saleur, Nucl. Phys. B **428**, 681 (1994); P. Fendley, Phys. Rev. Lett. **71**, 2485 (1993); P. Fendley, A. W. W. Ludwig, and H. Saleur, *ibid.* **74**, 3005 (1995); **75**, 2196 (1995).

[42] H. Frahm and A. A. Zvyagin, J. Phys. Condens. Matter **9**, 9939 (1997).

[43] A. A. Zvyagin, Phys. Rev. Lett. **79**, 4641 (1997).

[44] N. Oelkers, M. T. Batchelor, M. Bortz, and X.-W. Guan, J. Phys. A: Math. Gen. **39**, 1073 (2006).

[45] P. Schlottmann, Z. Phys. **54**, 207 (1984).

[46] P. Schlottmann, Z. Phys. **49**, 109 (1982).

[47] A. M. Tsvelick, J. Phys. C **17**, 2299 (1984).

[48] N. Kawakami, S. Tokuono, and A. Okiji, J. Phys. Soc. Jpn. **53**, 51 (1984).

[49] P. Schlottmann, Phys. Rep. **181**, 1 (1989).

[50] P. Schlottmann, Phys. Rev. B **36**, 5177 (1987).

[51] V. L. Pokrovsky and A. L. Talapov, Phys. Rev. Lett. **42**, 65 (1979); Zh. Eksp. Teor. Fiz. **78**, 269 (1980) [Sov. Phys. JETP **51**, 134 (1980)].

[52] While the Bethe *ansatz* cannot be formally applied to systems with inhomogeneous potentials along the chain, we expect that our findings will reveal themselves in different phases for the center of the tube and the end-points of the trap due to the renormalization of the the chemical potential caused by the harmonic confinement.[4] We believe this effect is generic for tubes of ultracold atoms.